Journal of the European Ceramic Society 17 (1997) 1877–1883

PII: S0955-2219(97)00069-1
0955-2219/97/$17.00 + 0.00

Corrosion Behaviour of Aluminium Nitride in Liquid Aluminium: Influence of the Microstructure

F. Roulet,[a] P. Tristant,[a] J. Desmaison,[a] R. Rezakhanlou[b] and M. Ferrato[c]

[a]Laboratoire de Matériaux Céramiques et Traitements de Surface, ESA CNRS 6015, Université de Limoges, 123 av. Albert Thomas, F-87060 Limoges, France
[b]EDF/DER/DEM, Centre de Recherche des Renardières, F-77250 Moret-sur-Loing, France
[c]Céramiques et Composites, Centre de Bazet, F-65460 Bazet, France

Abstract

The intrinsic characteristics of sintered aluminium nitride (mechanical, thermal, chemical) facilitate their use in production of heater element protection tubes for molten aluminium industries. Two kinds of industrial materials are characterised from the mechanical and thermal point of view. Moreover the samples' microstructure is observed before and after corrosion tests in liquid aluminium alloy (dipped finger method). The two batches exhibit identical mechanical properties and the thermal conductivity decreases from 170 Wm^{-1} K^{-1} at room temperature to 35 Wm^{-1} K^{-1} at 1000°C. Conversely, the distribution of the secondary phase (YAG) depends on the material. Despite the microstructure differences revealed by scanning (SEM) and transmission (TEM) electron microscopy, no corrosion is observed after 2000 h tests in molten aluminium alloy. These results confirm that AlN could be a good candidate for this application. © *1997 Elsevier Science Limited.*

Resumé

Les caractéristiques intrinsèques du nitrure d'aluminium fritté (mécaniques, thermiques, chimiques), permettent d'envisager son utilisation pour la réalisation de gaines protectrices de thermoplongeurs pour l'aluminium liquide. Deux nuances industrielles de cette céramique sont caractérisées d'un point de vue mécanique, thermique puis microstructural, avant et après essais de corrosion, dans un alliage d'aluminium fondu (méthode du doigt plongeant). Les propriétés mécaniques sont semblables pour les deux types d'échantillons, ainsi que la conductivité thermique qui diminue de 170 Wm^{-1} K^{-1} à l'ambiante à 35 Wm^{-1} K^{-1} à 1000°C. En revanche, la phase secondaire (YAG) est répartie différemment suivant la nuance. Indépendamment de la microstructure observée par microscopie électronique à balayage (MEB) et en transmission (MET) aucune différence de comportement n'est constatée pour des temps de contact avec un alliage d'aluminium allant jusqu'à 2000 h. Ces résultats confirment la potentialité de tels matériaux pour l'application visée.

1 Introduction

Aluminium nitride (AlN) is extensively used in the electronic industry for its many attractive properties including high thermal conductivity,[1–5] high strength,[6,7] a rather low thermal expansion[8] and other good electric properties.[9,10] Table 1 summarises these properties for AlN300, a commercial aluminium nitride from the Céramiques et Composites company (France). In addition, AlN exhibits an interesting chemical inertness towards some metals like aluminium. Indeed, a wettability test (by the sessile drop method) of liquid aluminium on hiped AlN substrates (relative density = 99·7%) for a non-isothermal run (up to 1200°C), has revealed a very limited attack (3 μm depth) in the centre of the reaction zone.[11] Such intrinsic characteristics mean this material has shown promising possibilities for molten aluminium industries. Applications in this field can involve many components

Table 1. Typical characteristics of AlN 300 from C&C company (France)

Typical characteristics (These properties are typical and should not be considered as specifications)		*Units*	
Physical	Crystal structure		Hexagonal
	Total porosity	% vol./% vol.	< 2·0%
	Apparent bulk density	10^4 kg m^{-3}	3·30
Thermal	Coef. of thermal expansion 20–100°C	10^{-6}°C^{-1}	3·2
	Thermal conductivity at 20°C	W m^{-1} K^{-1}	170
	Specific heat 20°C	J kg^{-1} K^{-1}	770
Mechanical	Vickers hardness (500 g load)	GPa	11
	Mechanical strength (4 points bending) at 20°C	MPa	300
	Weibull modulus at 20°C		10
	Klc Toughness at 20°C	M N m$^{-3/2}$	3·0
Electrical	Electrical resistivity	Ωm	> 1012
	Dielectric constant at 1 MHz		8·6
	Dielectric strength	kV mm^{-1}	> 15
	Maximum working temperature	°C	1200

which require high anti-corrosion behaviour, such as thermocouple and heater element protection tubes, riser stalk for low pressure cast, fitting pipe, gas injection pipe, ladle, shot sleeve and nozzle.

However, only pressureless sintering of AlN powder with additives, more frequently Y_2O_3, enables the industrial production of large size parts at a moderate cost. As no reaction is observed between pure AlN[11] and liquid aluminium, it is important to study the corrosion of pressureless sintered ceramic in order to establish the behaviour of the grain boundary secondary phase.

Therefore, the aim of the present work is to define, for two kinds of industrial AlN materials (C&C), the mechanical, thermal properties and the compatibility with a molten aluminium alloy by the dipped finger method. The sample microstructure is examined by scanning (SEM) and transmission (TEM) electron microscopy, before and after the corrosion runs.

2 Experimental

The samples investigated here are isostatic pressed cylinders (diameter = 10^{-2} m, length = 0.11 m) with Elf-Atochem spray-dried granules. The typical composition of this ready to press powder is shown in Table 2. Binders of the green body have been completely removed during the debinding step, by heat treatment in air at 600°C for 1 h. Two batches of AlN cylinders, AlN A and AlN B, have been sintered with the same sintering conditions (heating rate: 300°C h^{-1}, sintering temperature: 1800°C, dwell time: 3 h) but under different sintering atmospheres, influencing the material colour: AlN A is grey and AlN B is white.

The dipped finger method used for corrosion tests, has been conducted at the EDF Research Centre (Les Renardières). Ceramics were immersed for 1000 or 2000 h in alumina crucibles containing liquid aluminium alloy (AS7G0.6) at 800°C. Only the upper part (one third of the samples) stayed in the atmosphere of the furnace where argon dynamic flow was used in order to prevent aluminium liquid oxidation.

Table 2. Typical composition of ELF ATOCHEM (France) spray dried granules

Commercial grade	*Pyrofine ASD*
Typical composition	
Y_2O_3	3 wt% / AlN
Binders	4 wt% / AlN
Plasticizers	
Purity	
Oxygen	0·85%
Carbon	500 ppm
Iron	20 ppm
Silicon	50 ppm
Others	< 50 ppm

3 Results and Discussion

The mechanical and thermal characteristics do not reveal any pronounced difference between AlN A and AlN B (Table 3). The difference in colour of the two batches is not linked to the intrinsic characteristics of the materials.

On the contrary the electronic microscopy observations (SEM and TEM) show different distribution of the secondary phase (YAG: $Y_3Al_5O_{12}$).

3.1 Before corrosion tests

AlN A (colour grey): On the SEM cross section (Fig. 1) the matrix appears dark and from the

Table 3. Mechanical and thermal characteristics of the two batches of AlN

AlN	*Vickers hardness*		*σ_f(MPa) 3 point bending ($25\times4\times4\,mm^3$)*		*Thermal expansion coef. (K^{-1})*	*Thermal conductivity ($Wm^{-1}K^{-1}$) (error measurement 11%)*	
	H_v^{10N}	H_v^{200N}	*Before thermal shock**	*After thermal shock**	*(20–900°C)*	*T = 20°C*	*T = 1000°C*
A	1078 ± 22	1120 ± 36	416 ± 14	385 ± 13	$5{\cdot}4\ 10^{-6}$	170	30
B	1068 ± 21	1130 ± 31	373 ± 13	384 ± 13	$5{\cdot}4\ 10^{-6}$	170	40

*Thermal shock: samples introduced in a furnace at 800°C then cooled at the rate of $10°C\,min^{-1}$.

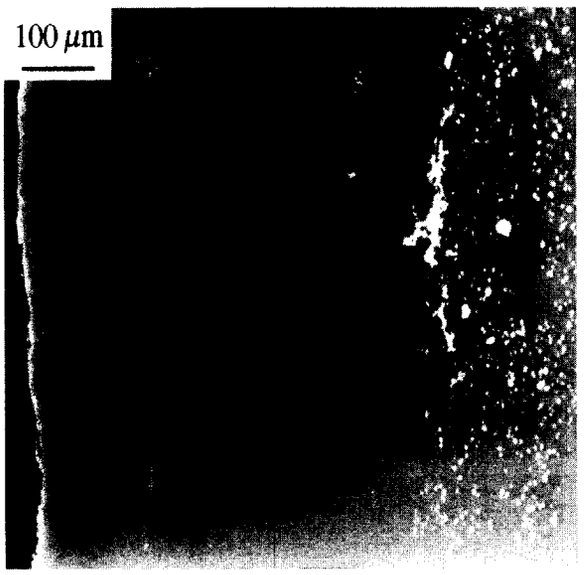

Fig. 1. SEM cross section of AlN A.

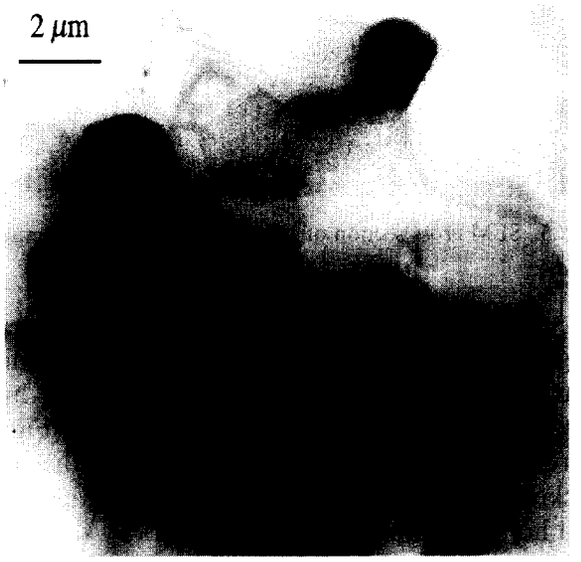

Fig. 3. TEM micrograph of the inner part of AlN A.

external side (200–400 μm thick) the YAG phase is detected in very small amounts (pale spots). Conversely, the TEM micrograph shows the secondary phase as dark (in comparison with AlN grains) which are localised in pockets at the grain boundaries (Fig. 2). Beyond this zone, the YAG phase reappears as individual grains homogeneously distributed (Fig. 1) which is revealed as dark grains in Fig. 3.

AlN B (colour grey–white): In the same sample, two microstructures can be observed. The first one is identical to that of AlN A with almost no YAG phase in the 350 μm thick external region (Fig. 4). However, the second one is more heterogeneous

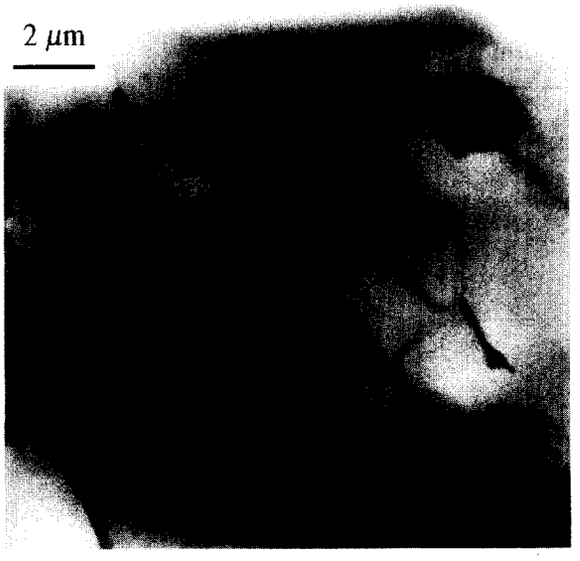

Fig. 2. TEM micrograph of the external side of AlN A.

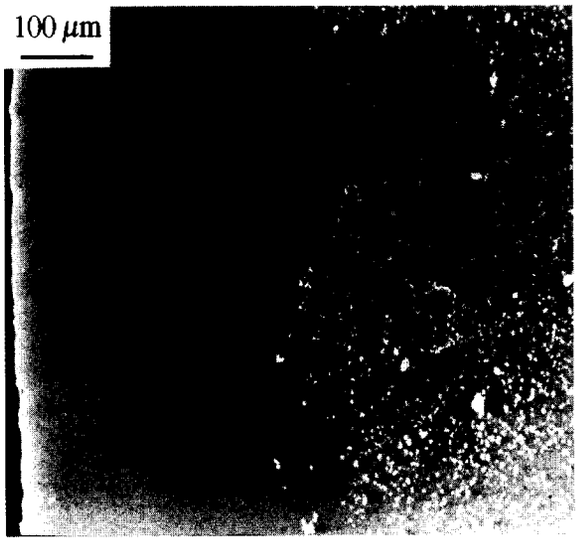

Fig. 4. SEM cross section of AlN B (first microstructure, identical to AlN A).

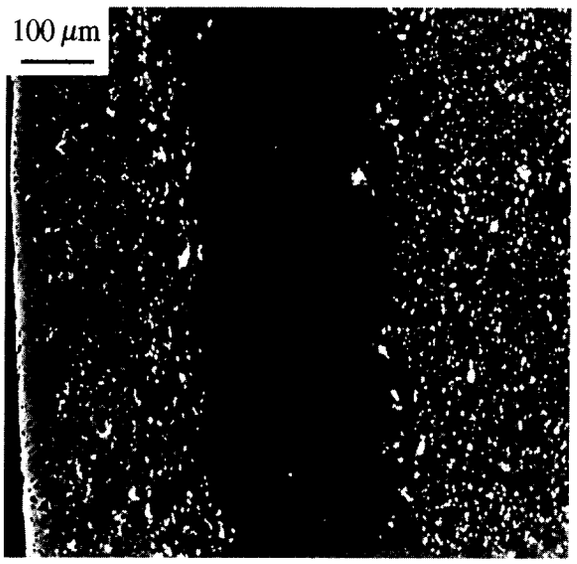

Fig. 5. SEM cross section of AlN B (second microstructure).

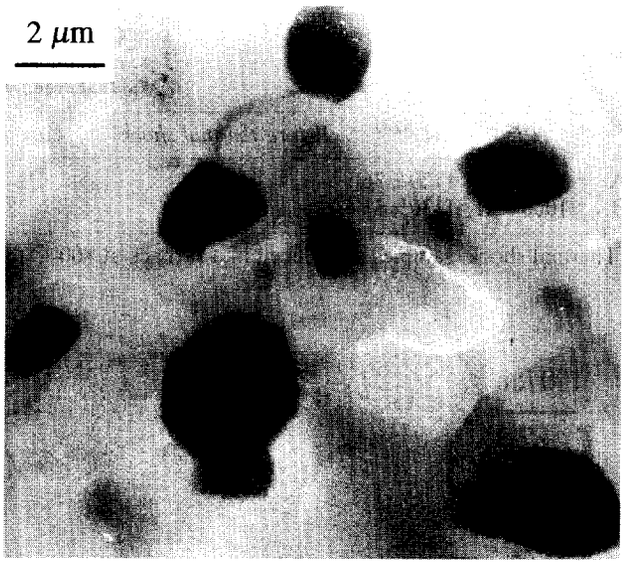

Fig. 7. TEM micrograph of the inner part of AlN B.

(Fig. 5). Starting from the surface, a 200 μm thick zone, rich in the secondary phase exhibiting high porosity and rounded AlN grains, is observed (Fig. 6) in front of a depleted zone of approximately the same thickness (≈200 μm). The inner part is characterised by a homogeneous distribution (Fig. 7).

3.2 After corrosion tests

The SEM observation of the surface of AlN A, immersed for 1000–2000 h in liquid aluminium alloy, reveals no corrosion (Fig. 8) either in the matrix or in the secondary phase. This result is corroborated by TEM observations which also show no aluminium penetration, with no modification of the microstructure in the external part of the sample, as demonstrated in Fig. 9, which is similar to the Fig. 2 (before corrosion test).

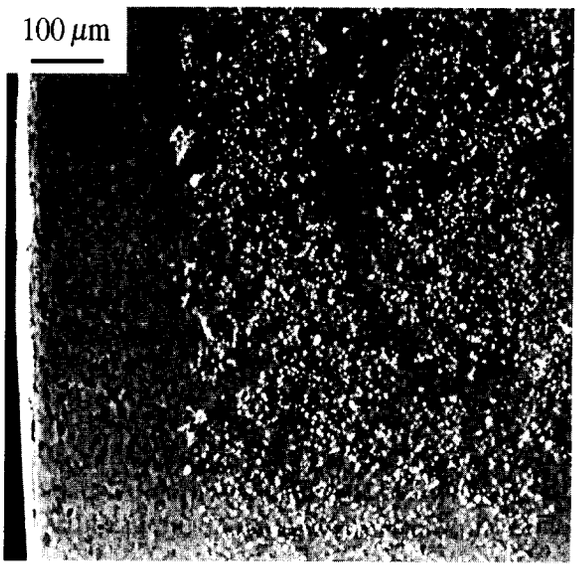

Fig. 8. SEM micrograph of the AlN A/Al interface, after corrosion test for 2000 h.

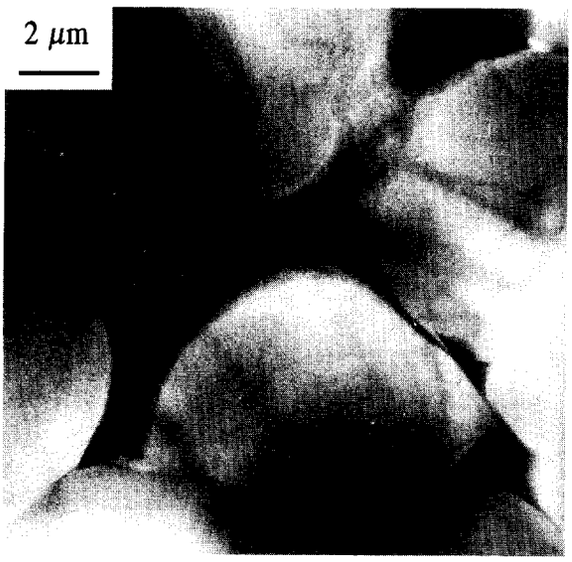

Fig. 6. TEM micrograph of the external side of AlN B.

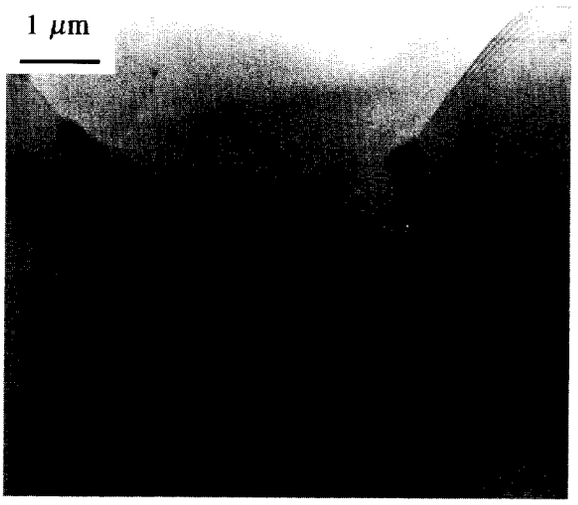

Fig. 9. TEM micrograph of the external side of AlN A, after corrosion test for 2000 h.

Despite a rich zone in the secondary phase and porosity near the surface, AlN B appears no more corroded on both the SEM and TEM observations (Figs 10 and 11, respectively), after tests for 1000 or 2000 h, in comparison with the microstructure before corrosion described in Figs 5 (SEM) and 6 (TEM), respectively.

An EDX analysis (STEM mode) of the two samples (immersed for 1000 or 2000 h) illustrates the same behaviour. Therefore, this work only describes the results obtained for AlN A tested for 2000 h.

Figure 12(a) is a TEM micrograph of the region near the AlN A/liquid aluminium alloy interface which shows YAG inclusions (dark zones) in the matrix (pale zones). The element maps of this region reveal different impurities in the secondary phase, like Zn, Si, distributed throughout the observation zone [Fig. 12(b) and (c), respectively]. These elements originated in the AlN powder and are trapped in the secondary phase like most of the other metallic impurities. The argon in Fig. 12(d), which originates from the ionic bombardment used in the last step of sample thinning, seems to be introduced more easily in the matrix than in the YAG phase (pale zones are more concentrated).

Using this analysis technique, an important contrast is revealed for the yttrium map which is more abundant in the YAG phase. On the other hand, analysis of the light atoms is always difficult. The oxygen [Fig. 12(f)] seems to be more abundant in the secondary phase but can be revealed only in important YAG pockets. The nitrogen map is still less clear [Fig. 12(g)], but different pale zones (less concentrated) appear in the YAG inclusions.

In respect of aluminium, precautions must be taken for interpretation of the results. A simple calculation of the Al content in pure YAG and AlN phase from the molecular weight and the density, gives a higher wt% of Al in the matrix (around 23 and 66% in $Y_3Al_5O_{12}$ and AlN, respectively). So, it is normal that the element map [Fig. 12(h)] shows a less concentrated (dark zones) secondary phase in comparison with the uniform distribution (pale zones) of the matrix.

In order to establish the corrosion resistance of AlN, the Al content in the secondary phase inclusion must be compared with a map before corrosion. Figure 13(a) which is a SEM micrograph of AlN A before testing, points out the YAG phase where the yttrium and aluminium distributions [Fig. 13(b) and (c)] are determined by means of an energy dispersive (EDX). As the pale zones are more concentrated, the yttrium appears in the inclusion where Al is less abundant.

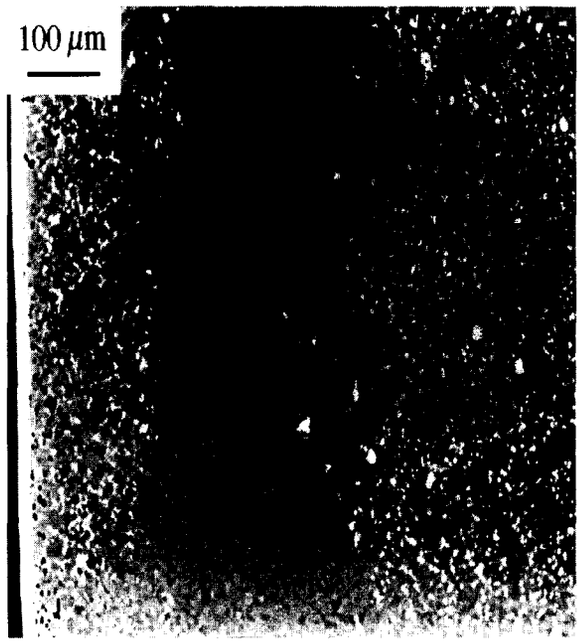

Fig. 10. SEM micrograph of the AlN B/Al interface, after corrosion test for 2000 h.

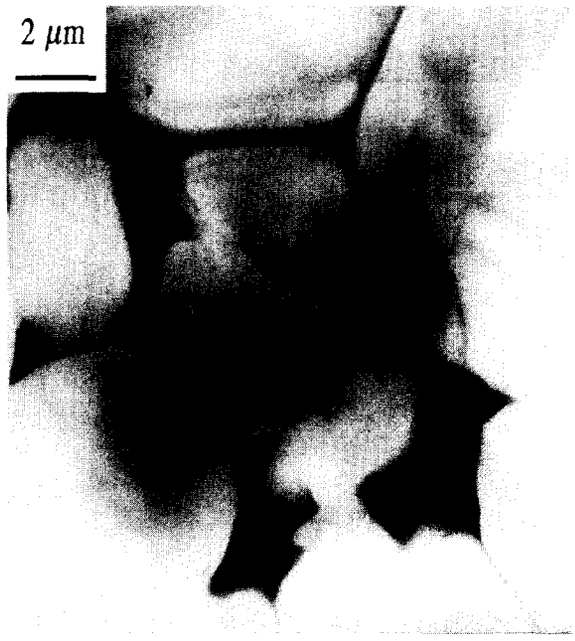

Fig. 11. TEM micrograph of the external side of AlN B, after corrosion test for 2000 h.

These results are typical for sintered AlN with additives (Y_2O_3):

—Y, Al, O (elements of the YAG phase) and different metallic impurities in the secondary phase,

—N and much Al in the matrix,

and show no secondary phase enrichment in aluminium during the corrosion tests. This conclusion explains why no corrosion has occurred.

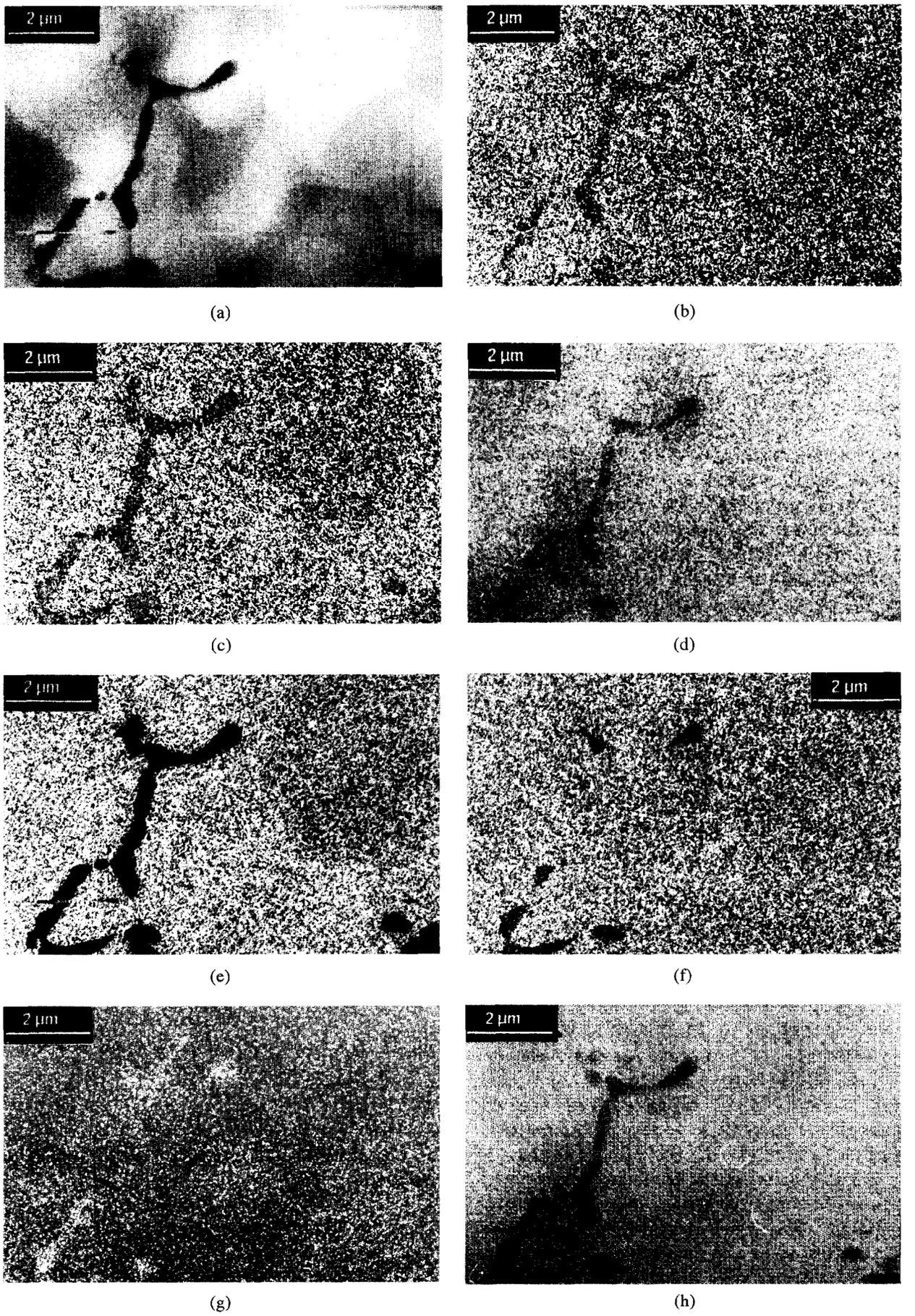

Fig. 12. Elements maps (EDX) of the external side of AlN A after corrosion test (2000 h). (a) TEM micrograph of the analysed zone; (b)–(h) individual maps of Zn, Si, Ar, Y, O, N and Al, respectively; NB: (b), (c), (e), (f), (g) the dark zones are more concentrated than the pale zones: (d), (h) the dark zones are less concentrated than the pale zones.

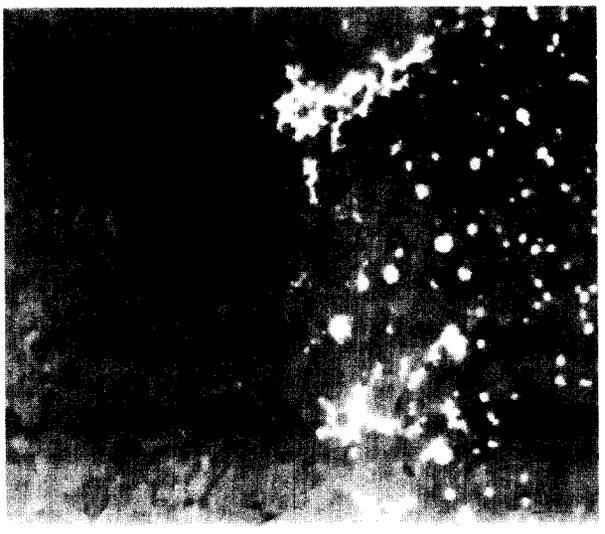

(a)

(b)

(c)

Fig. 13. Elements maps (EDX) of the external side of AlN A before corrosion test. (a) SEM micrograph of the analysed zone; (b), (c) individual maps of Y and Al, respectively. (The dark zones are less concentrated than the pale zones).

4 Conclusion

Despite microstructure differences, the two kinds of commercial AlN present similar mechanical and thermal properties. In addition, even if the thermal conductivity decreases to about 30–40 $Wm^{-1}\ K^{-1}$ at the working temperature of heater elements, these values are very interesting in comparison with other ceramics. Moreover, the results obtained by the dipped finger method, corresponding to long term corrosion tests, are very similar to real conditions and clearly show the good resistance of sintered AlN with yttrium additives. Therefore, these industrial ceramics could be good candidate materials for protective tubes for the handling or melting of liquid aluminium or liquid aluminium alloys.

References

1. Buhr, H. and Muller, G., Phase composition, oxygen content and thermal conductivity of AlN (Y_2O_3) ceramics. *Journal of the American Ceramic Society*, 1991, **74** (4), 718–723.
2. Haase, I. and Himpel, G., Development of single phase aluminium nitride ceramics. *ECERS Conference III rd Euro-Ceramics*, Vol. 1, eds P. Duran and J. F. Fernandez. Madrid, 1993, 943–948.
3. Lee, R. R., Development of high thermal conductivity AlN ceramic. *Journal of the American Ceramic society*, 1991, **74** (9), 2242–2249.
4. Lee, W. E., Chiang, S. K., Readey, D. W., Donn, R. and Shaffer, P. T. B., Relation between thermal conductivity, sintering mechanism and microstructure of AlN with yttrium aluminate grain boundary phases. *Journal of Materials Science and Electronics*, 1992, **3**, 93–101.
5. Mullot, J., Contribution à l'étude de l'évolution de l'oxygène et de la microstructure dans les substats de nitrure d'aluminium à forte conductivité thermique frittés en présence du fluorure d'yttium. Thesis of the University of Limoges, 1995.
6. Savrun, E. and Lougher, W., Surface finish effects on metallization of aluminium nitride substrates. *Ceramics Transactions*, 1993, **15**, 583–602.
7. Boch, P., Glandus, J. C., Jarrige, J., Lecompte, J. P. and Mexmain, J., Sintering oxidation and mechanical properties of hot-pressed aluminium nitride. *Ceramics International*, 1982, **8**(1), 34–39.
8. Yim, W. M. and Pafe, R. J., Thermal expansion of AlN, sapphire and silicon. *Journal of Applied Physics*, 1974, **45**(3), 1456–1457.
9. Prohaska, G. W. and Miller, G. R., Aluminium nitride: a review of the knowledge base for physical property development. *Materials Research Society Symposium Proceedings*, 1990, **167**, 215–227.
10. Zulfequar, M. and Kumar, A., Electrical conductivity and dielectric behaviour of hot-pressed AlN. *Advances in Ceramic Materials*, 1988, **3**(4), 332–336.
11. Mouradoff, L., Tristant, P., Desmaison, J., Labbe, J. C., Desmaison-Brut, M. and Rezakhanlou, R., Interaction between liquid aluminium and non-oxide ceramics (AlN,-Si_3N_4 SiC). *Key Engineering Materials*, 1996, **113**, 177–186.